

Received August 24, 2021, accepted September 12, 2021, date of publication September 20, 2021, date of current version October 27, 2021.

Digital Object Identifier 10.1109/ACCESS.2021.3114226

An Improved Agent-Based Model Using Discrete Event Simulation for Nonpharmaceutical Interventions

HONGBIN QIU^{ID}, YONG CHEN^{ID}, SIRUI DING, WENCHAO YI^{ID}, (Member, IEEE),
RUIFENG LV, AND CHENG WANG^{ID}

College of Mechanical Engineering, Zhejiang University of Technology, Hangzhou 310014, China

Corresponding author: Wenchao Yi (yiwenchao@zjut.edu.cn)

This work is supported by National Natural Science Foundation of China under Grant 52005447, and in part by the Zhejiang Provincial Natural Science Foundation of China under Grants LQ21E050014, Y16G010038 and LY18G010020.

ABSTRACT The traditional agent-based model requires high computing power of the central processing unit. Thus, an improved agent-based model combined with the discrete event simulation method is proposed. The result of the equation-based Susceptible-Exposed-Infective-Asymptomatic-Recovered (SEIAR) model with the same parameter combination, which has been demonstrated to be effective, is used to verify the validity of this improved agent-based model. Additionally, an analysis based on simulation results of the Contact Tracing Measure (CTM), Location-Based Checking-Testing Measure (LCTM), Lockdown Measure (LM), Mobile Cabin Isolation and Hospital Measure (MCHM) is presented. The simulation results show that implementing long-term lockdown measures has the best effect on epidemic control. Moreover, according to the simulation results, we inferred that using only nonpharmaceutical epidemic prevention measures may result in a second outbreak of COVID-19 owing to the risk of asymptomatic transmission.

INDEX TERMS Agent-based model, asymptomatic, COVID-19, discrete event simulation.

I. INTRODUCTION

Since December 2019, severe acute respiratory syndrome corona virus 2 (SARS-CoV-2), which causes the disease called COVID-19, has spread in Wuhan, China. COVID-19 has now spread globally, which has caused a huge number of civilian deaths and economic losses [1]. According to statistics from the Center for Systems Science and Engineering (CSSE) at Johns Hopkins University (JHU), as of 16 December 2020, the number of confirmed COVID-19 cases worldwide had reached 73,475,980, and the death toll was up to 1,635,427 [2]. On the 11th of March 2020, the World Health Organization declared COVID-19 a pandemic, and the countries at risk were advised to strengthen countermeasures. Hence, developing methods to simulate the evolution of this epidemic has become a mainstream trend to help governments formulate effective and timely prevention and control strategies [4].

The associate editor coordinating the review of this manuscript and approving it for publication was Xiwang Dong.

Generally, disease modeling approaches include ordinary differential equations (e.g., the Susceptible-Exposed-Recovered (SIR), Susceptible-Exposed-Infective-Recovered (SEIR) models) to estimate infection spread [5]; system dynamics methods, which rely on mechanisms, such as stocks, flows, internal feedback loops, table functions and time delays [6]; and data-driven modeling to estimate the fatality ratio across the spectrum of COVID-19 disease [7]. System dynamics methods have been shown to adequately and extensively capture the overall dynamics of a disease outbreak [38].

In recent years, the agent-based model (ABM) has become a research hotspot. The ABM is a type of computational model in which each agent makes decisions based on a set of rules within an environment specified by the users [9]. Additionally, it allows users to identify how and why a given set of interactions among individuals generates some collective results [10]. Moreover, the ABM helps when studying complex adaptive systems through systematic abstraction of the systems using a bottom-up approach. It is especially

amenable to incorporating detailed, multilayered empirical data on human behavior, as well as social and physical environments. The ABM can also represent granular information, which is not easily managed with statistical/mathematical models [11]. Moreover, the model can incorporate a wide range of empirical measures, including but not limited to age-specific mortality, fertility, poverty, disease risk, demographic composition, preferences, behaviors and so on [12].

Thus far, researchers have applied the ABM to simulate the spread of infectious diseases. Merler *et al.* [13] modeled the movements of individuals using the ABM, i.e., seeking assistance in health care facilities, the movements of individuals taking care of patients infected with Ebola virus who were not admitted to hospital, and the attendance of funerals. Mahmood *et al.* [14] extended the traditional SEIR model and proposed an ABM to analyze interactions between a host and a vector such that the spread of a disease in a given area over time can be forecasted. Hunter *et al.* [15] used open data and created a data-driven ABM to simulate the spread of an airborne infectious disease in 33 different Irish towns to study the correlations between the simulation results and the town characteristics (i.e., the population, area and age structures). Crooks and Hailegiorgis [16] used data from a refugee camp and geographic information science (GIS) elevation data for an ABM on the spread of cholera. Waleed *et al.* [18] presented an agent-based simulation engine that uses human-to-human interactions, population dynamics, disease transmissibility and disease states as inputs, which can model the spread of infectious diseases in a population. Gopalan and Tyagi [21] developed an agent-based simulation framework in Python and used it to compare the performance of three testing policies, i.e., Random Symptomatic Testing (RST), Contact Tracing (CT), and a new Location-Based Testing (LBT) policy. Notably, however, their models all run in supercomputing centers.

Actually, “agent-based models are computationally intensive” is industry-recognized [13]–[20], [38], [39], which is the primary reason for the work presented in this paper. In terms of the nature of the model, an ABM is a pseudodistributed system [27], i.e., it is a collection of objects that are concurrently active and communicate with each other (despite the concurrency being simulated by the engine). The internal dynamics of the agent can be best captured using system dynamics or the discrete event approach [34], [37]. Thus, in Section III, an improved ABM combined with the discrete event simulation (DES) method is presented. In the proposed model, agents are considered entities during the process; this process will replace the original transition processes. With the same scenario and population size, a traditional agent-based simulation model is difficult to apply using a desktop computer with the following specifications: Intel(R) Core (TM) i5–10600KF CPU @4.10 GHz, 16.0GB RAM, and GeForce GTX 1660 SUPER GPU, but the improved agent-based simulation model can easily be run on the same desktop. In addition, we can extend the improved simulation model by considering many nonpharmaceutical

interventions with the above desktop. After verifying the validity of this improved model in Section III, the quantification and assessment of the influence of the Contact Tracing Measure (CTM), Location-Based Checking-Testing Measure (LCTM), Lockdown Measure (LM), Mobile Cabin Isolation and Hospital Measure (MCHM) are given in Section IV. Finally, future research directions and conclusions are presented in Section V.

II. TEST SUITE AND PARAMETERS

For reasons of limited computational power in the laboratory, we can select a university campus at Hangzhou (China) as the research object of our model and assume that patients with COVID-19 are present on this campus. Although the agent-based simulation model is improved, high concurrency is an essential characteristic of the model. The high demand for computing power is still a disadvantage of the model in large-scale applications. Additionally, due to the regional isolation experience in China, we study the proposed model at the university scale. We obtain geographic information about this campus from Google Earth, i.e., the spatial distance data, the distribution of different buildings, specification features, and the dimensions of these structures on campus.

A. DESCRIPTION OF THE TEST SUITE

To make the simulation model more realistic, we collect the population data of this campus using the admissions website. The male-female ratio is approximately 1:1.

TABLE 2 shows the data of undergraduates in different majors and grades, which are available online [36]. TABLE 1 presents the structural information of doctoral and master’s degree candidates in different majors and grades. The data are also available online [37]. Through TABLE 1 and TABLE 2, we can clearly know the number of students in different majors and grades within this campus area and the total number of students.

TABLE 1. The structural data of doctoral and master graduates.

SPECI ALTY CODE	2019D	2020D	2018M	2019M	2020M	IN THIS CAMP US
1	53	56	389	400	564	NO
2	29	32	361	372	525	YES
3	15	16	284	296	364	NO
4	27	26	114	193	213	YES
...
17	0	0	72	57	101	NO
18	0	0	32	31	34	YES
SUMM ARY	212	243	2864	2963	4077	

Three details of this table must be considered: (a) we do not consider part-time postgraduates, (b) specialty codes 4 and 20 belong to the same specialty before 2020, which is why codes 2019D, 2018M and 2019M are 0, (c) 2019D corresponds to a doctoral candidate in 2019, and 2018M corresponds to a master’s degree candidate in 2018.

Three details of this table must be considered: (a) we do not consider part-time postgraduates, (b) specialty codes 4 and 20 belong to the same specialty before 2020, which

TABLE 2. The structural data of undergraduates.

SPECIALTY CODE	2017	2018	2019	2020	IN THIS CAMPUS
1	80	81	84	84	YES
2	59	60	62	62	YES
3	140	143	148	148	YES
4	284	289	299	299	NO
5	674	684	708	708	YES
6	187	190	196	196	YES
7	828	841	870	871	NO
8	215	218	226	226	NO
9	219	222	230	230	YES
10	174	177	183	183	YES
11	400	406	420	421	YES
12	855	868	898	899	NO
13	178	180	187	187	YES
14	297	301	312	312	YES
SUMMARY	4589	4660	4821	4826	

“Specialty Code” is the mark for various students from different specialties. We divide these undergraduates into different groups according to specialty and grade (similar to a series of rules for building the database for undergraduates where “Specialty Code” is one of the rules). In addition, we screened out and deleted the students who did not belong to this campus from the database using the 6th column (named “in this campus”).

is why codes 2019D, 2018M and 2019M are 0, (c) 2019D corresponds to a doctoral candidate in 2019, and 2018M corresponds to a master’s degree candidate in 2018.

“Specialty Code” is the mark for various students from different specialties. We divide these undergraduates into 14 × 4 different groups according to specialty and grade (similar to a series of rules for building the database for undergraduates where “Specialty Code” is one of the rules). In addition, we screened out and deleted the students who did not belong to this campus from the database using the 6th column (named “in this campus”).

B. BEHAVIORAL PATTERNS OF STUDENTS

As mentioned above, the ABM has advantages related to individual behavioral patterns and feature modeling of population structures (age, gender and so on). In general, infectious disease spread is based on social interactions between individuals. When healthy and infectious individuals have close contact in the same space (the contact is considered effective

once the distance between individuals is less than a certain radius within which the virus will spread), healthy individuals are at risk of being infected. The rules of individual space state transitions are simulated by modeling the behavioral patterns of the groups.

In fact, a behavior pattern refers to the daily route of each agent [29], [39]. As most of the ABS model uses agents’ daily routine data to realize the transfer and interaction of agents in geographical space, this model is also adopted in this paper. The database shows how much time every student spends in each place and how each agent interacts with other agents in the enclosed area. For the case studied in this paper, an agent represents a student, and the number of student groups equals the number of related agent groups. In a certain agent group, each agent contains the information about which dorm he is in and which building a class is in. This information is determined by his grade and major. Depending on his major and grade, he will be at different places at different times. Generally, students in different grades and majors will have different behavior patterns, while female/male students in the same grades and majors will share the same behavior pattern. Information about the dormitory where each student lives, the building where each student studies in the morning/afternoon/evening, and the possible places that most of the students choose when they are idle in the morning/afternoon/evening are collected. Agents in different groups have different genders, majors and grades. The students (agents) can be divided into 2 groups based on gender. Both males and females can be divided into 9 groups according to their grades. There are 22 colleges for undergraduates, 19 major enrollments for postgraduates and 4 major enrollments for doctoral candidates. Hence, all students in this campus are divided into 236 groups, which have different populations and behavioral patterns (our university has four campuses in different places).

The space state transition information is presented in TABLE 3 (only part of the full table is presented owing to page limitations). As we can see from this table, the identity code for each student is defined according to their gender, major, and grade. The code is used for simplicity in the table. The information was collected through questionnaires and other mechanisms; then, we summarized the behavioral

TABLE 3. The space state information of different crowds.

CODE FOR IDENTITY	QUANTITY	MORNING CLASS LOCATION	AFTERNOON CLASS LOCATION	EVENING CLASS LOCATION	DORMITORY FOR BOY STUDENTS	DORMITORY FOR GIRL STUDENTS
10101	80	JXA	GZB	JXB	DE9	DW4
10102	59	BYA	CY	GZC	DE12	DW6
10103	140	YWA	GZA	JXA	DE15	DW14
10105	674	YWB	JXB	JXA	DE11	DW14
...
20927	26	JXA	GZB	ME	DE5	DW14
20928	140	Random	Random	ME	DE12	DW6
20932	34	Random	IE	IE	DE12	DW2
20934	49	CST	IE	Random	DE16	DW1

patterns into different groups. In particular, when agents are created (also the entities in discrete events) by querying the database, the behavioral patterns of every group are distinguished based on an identity code. Finally, the state chart library of Anylogic software was used to model these students' behavioral patterns (Fig. 1).

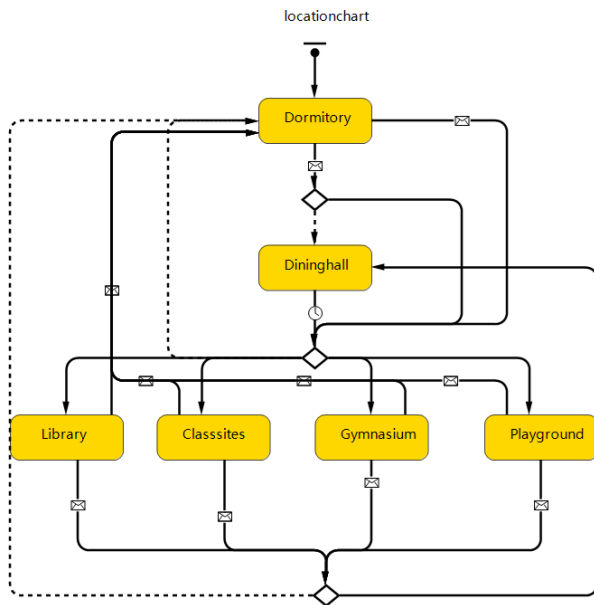


FIGURE 1. A chart of students' locations (which is an abstraction of their behavioral patterns).

C. VITAL PARAMETERS

A successful simulation model requires fine-tuned parameters to present matching simulation results. The related parameters are determined by means of literature and historical databases, which are given in TABLE 4.

D. MODEL ASSUMPTION AND EXPLANATION

The ABM using the discrete event simulation method is proposed due to its industry recognition [13]–[20], [38], [39].

In addition, some assumptions must be established for the model to run legitimately, as follows:

- 1) Each person who has not been infected by COVID-19 is in the susceptible state.
- 2) Each agent can be infected only once, indicating that the recovered agents can remain healthy until the simulation ends. Agents who are pronounced dead are immediately removed from the population.
- 3) The initial number of patients is set to 3. If a patient is within the university or community, the Chinese government will lock down the whole area for isolation.
- 4) The simulation step is 1 day, and the total running time of the simulation model is 100 days.
- 5) All students are assumed to follow their own routine schedule, which will ensure that we can determine that

the behavior pattern of each agent group relies on their routine schedule.

III. IMPROVED ABM WITH THE DES METHOD

Two-state transition models—the abstraction of the disease transmission process and the space state transmission process in homologous geographic areas—are the fundamental preconditions of an integrated ABM [12], [34]. In an ABM, the system may interact with each itself and the environment, leading to concurrent subsystems. The bottom-up approach implies that we need to abstract the state transition of the agent and then duplicate it, which will lead to high concurrency [9], [12], [34]. In infectious disease simulations, the ABM will simulate the real situation of society. Therefore, the social structure, population size, behavioral patterns of people in the GIS data, and even their mental states will be considered when building the model. Hence, the computing power demand of the ABM is too high for the infectious disease spread field. Thus, an improved ABM, which is combined with the DES method, is proposed to address the issues described above.

A. THE IMPROVED MODEL

The proposed multimethod ABM is built using Anylogic software [35]; here, we present the modeling process using the logic and modules of this software. The ABM is usually built with a state chart library. The state transition is triggered by messages, time clocks or condition functions, and the different states indicate different possible space locations. Here, the process chart library replaces the state chart library, and the interaction between the illness chart and discrete event model parts is created by some other variables. In the improved model, agents act as entities in a process from beginning to end. The information of every agent, including gender, behavioral patterns and age distributions, is stored in a series of databases and is mapped to every agent when the model starts running. Every entity in the process has an agent linked to it, and vice versa. The whole process is divided into different subprocedures on the basis of geographical features. The agents interact with each other in different manners, e.g., the infection probability or response per day, which both depend on the type of every subprocedure. Fig. 2 presents a comparison between the pure ABM and the improved ABM with the DES method.

The space state features and interaction processes of entities in this specific region are implemented using the process chart library. The interactions among agents and between agents and the environment are still implemented with the state chart library during susceptible-exposed-symptomatic-untreated-recovered processes. Throughout the design of ABMs, the following aspects should be noted:

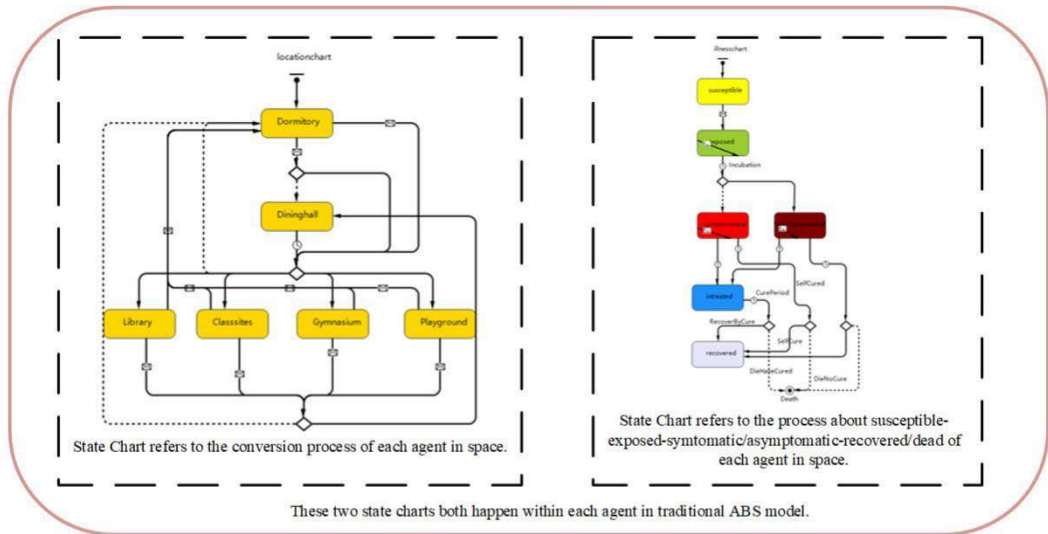
The send message module is always used as the major interactive method for disease transmission in the model, whether the traditional or the improved ABM. The difference is that the indicator triggering interaction is the state information of every agent in the classical ABM. The extra

TABLE 4. The parameters related to disease.

NAME OF THE PARAMETER	EXPLANATION OF THE PARAMETER	INITIAL VALUE	REFERENCES/DATA SOURCES
N	The total number of students in this campus (also the number in this agent group).	17782	Actual Statistics
S	The number of susceptible individuals.	17779	Self-defined
I	The number of symptomatic individuals.	3	Self-defined
R	The number of recovered individuals.	0	Self-defined
A	The number of asymptomatic individuals.	0	Self-defined
E	The number of exposed individuals.	0	Self-defined
D	The number of deceased individuals.	0	Self-defined
T	The number of students treated in a hospital/clinic.	0	Self-defined
ϵ	The probability of spreading the disease successfully through contact with exposed individuals.	0.01	[23], [31], [32]
β	The probability of spreading the disease successfully through contact with symptomatic individuals.	0.07	[31], [32], [47]
α	The probability of spreading the disease successfully through contact with asymptomatic individuals.	0.035	[25], [31]
ω'	The inverse of the duration from exposure to asymptomatic disease.	$\frac{1}{\text{Triangular}(3,14) \text{ days}}$	[26], [27]
ω	The inverse of the duration from exposure to symptomatic disease.	$\frac{1}{\text{Triangular}(3,7) \text{ days}}$	[26], [27]
$t_{self-cure}$	The period relying on own immune system for recovery.	Triangular (14,27) days	[24]
$t_{cure-by-treating}$	The period from admission to recovery and discharge.	Triangular (9,14) days	[27]
γ	The probability of recovery for symptomatic individuals relying on their own immune system for recovery.	0.962	[47], [48]
γ'	The probability of recovery for asymptomatic individuals relying on their own immunity system for recovery.	0.981	[47], [48]
ρ	The probability of recovery for patients treated in the hospital.	0.9934	[47], [48]
n_{class}	The average contact number of people per student when attending class.	40	Actual Statistics
$n_{quarantine}$	The average number of close contacts per student in quarantine.	0	Actual Statistics
$n_{dormitory}$	The average contact number of people per student in dormitories.	10	Actual Statistics
$n_{empty-spaces}$	The average number of close contacts per student in empty spaces.	8	Actual Statistics
p	The probability of exposed individuals to asymptomatic individuals.	0.14	[27]
$t_{isolation}$	The duration of isolation for those with suspected infection.	15 days	[35]
t_{NAT}	The days required for nucleic acid testing (which depends on the local medical level).	Triangular (0.5,1) days	Actual Statistics
$n_{dining\ hall}$	The average number of close contacts per student within the dining hall.	30	Actual Statistics
b_{tc}	The COVID-19 test success rate.	0.8	Self-defined
$c_{isolation}$	The capacity of the quarantine facility.	100	Actual Statistics
c_{treat}	The capacity of the clinic/hospital.	50	Actual Statistics

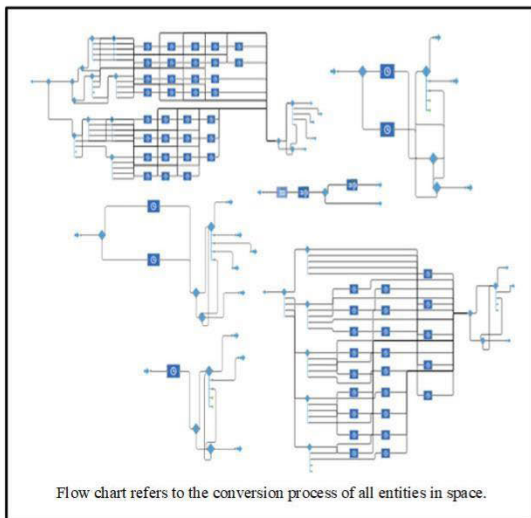
variable indicating entities' space state information is added in the improved ABM with the DES method. The reason is that the process of space state transition is external in the improved model; thus, an additional intermediary linking the homologous agents for feedback on external space states information is necessary.

The improved ABM with the DES method performs better regarding model fitness. The accuracy of the 2D grid map is not as good as that of the GIS map, which leads to deviation in the space distance and dimensional error of architectures; the accuracy can be easily improved through parameterization and discretization. With regard to parameterization and



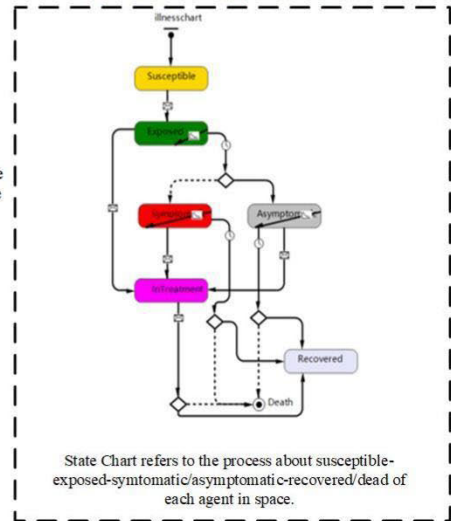
Improving agent-based model by combination with discrete event simulation method.

This flowchart happen for the whole entities, not within any agent.



The additional intermediary links the homologous agents for feedback the external space states information.

This state chart still happen within each agent.



Flow chart happens for the whole entities, while the state chart happens within each agent.

FIGURE 2. Comparison between the pure ABM (left) and the improved ABM with the DES method.

discretization, the whole process is split in terms of location differences by modularization. Accordingly, the detailed process of every entity in various locations and the parameters describing the whole process (such as the delay time, a series of possible epidemic prevention measures, other entities moving in the same place, the number of contacts per day and several other significant factors) can be abstracted out. With sufficient computing power, the interaction processes between agents and their environment can be simulated and described in detail.

Due to high concurrency, the classical ABM could not be run on the desktop; however, this was not the case with the

improved ABM (with the DES method). The DES method can effectively reduce the number of concurrent agents, which is not the case with the pure ABM that can only be run in a supercomputing center. Namely, the demand for computing resources of the improved ABM with the DES method is less than that of the traditional ABM with the same parameter combination.

B. SEIAR EQUATION-BASED MODEL (WITHOUT INTERVENTION)

The validity of the equation-based susceptible-exposed-infected-asymptomatic-recovered (SEIAR) model has been

proven, and it is also widely applied in the disease prevention and control field [32], [43]. The mathematical model of the SEIAR model (without intervention) is presented as follows. Detailed parameters and the corresponding values and explanations are given in TABLE 4.

$$dS/dt = -\beta \cdot S \cdot I - \alpha \cdot S \cdot A - \varepsilon \cdot S \cdot E \quad (1)$$

$$dE/dt = \beta \cdot S \cdot I + \alpha \cdot S \cdot A + \varepsilon \cdot S \cdot E - (1-p) \cdot \omega \cdot E - p \cdot \omega' \cdot E \quad (2)$$

$$dI/dt = (1-p) \cdot \omega \cdot E - \gamma \cdot I \quad (3)$$

$$dA/dt = p \cdot \omega' \cdot E - \gamma' \cdot A \quad (4)$$

$$dR/dt = \gamma \cdot I + \gamma' \cdot A \quad (5)$$

C. VALIDATION OF THE MODEL

The improved ABM combined with other simulation methods has been studied. Marilleau *et al.* [40] coupled agent-based equation-based models (EBMs) to study spatially explicit megapopulation dynamics in 2018. Rakowski *et al.* [17] compared the results of an ABM with the results of the SIR differential equation model, and the matching trend illustrates the validity of the model. Skvortsov *et al.* [41] demonstrated that the validation of an ABM can be verified using simple mathematical models, and the classical SIR model is used as an example. Connell *et al.* [42] obtained a similar result by different methods.

To validate the effectiveness of the proposed model, a SEIAR model is established with the same parameters as this improved ABM model without taking any intervention measures. The proposed model is carried out on a desktop with the following specifications: Intel(R) Core (TM) i5-10600KF CPU @4.10 GHz, 16.0GB RAM, and GeForce GTX 1660 SUPER GPU, and the Anylogic software version is Professional 8.7.4. The proposed simulation model can be accessed through the website <https://github.com/qihongbin981247/Anylogic.git> for academic use.

As shown in Fig. 3, for the same type of population, the simulation results show that the changing trend is basically the same for the compared group [12]. The SEIAR model approximates the data with a smooth function through the underlying analytical form, and the results are calculated based on the model parameters; however, the ABM allows reproduction of the nonsmooth behavior [40]–[42]. Hence, evaluating the similarity between the ABS model and the SEIAR EB model is evident on a qualitative level in most cases, which matches the overall resulting curves [8], [17], [36].

Fig. 3 shows that the rapid spread and outbreak of the epidemic basically occurred within a duration of 10–50 days. Comparatively, the result of the ABS model seems more optimistic. In the improved ABS model, the outbreak peak is later, and the peak is higher. In addition, according to the simulation results of the improved ABS model, the epidemic ends earlier, and more people eventually achieve recovery. In particular, the number of asymptomatic patients in the improved ABS model seems greater than that in the EB model. A higher

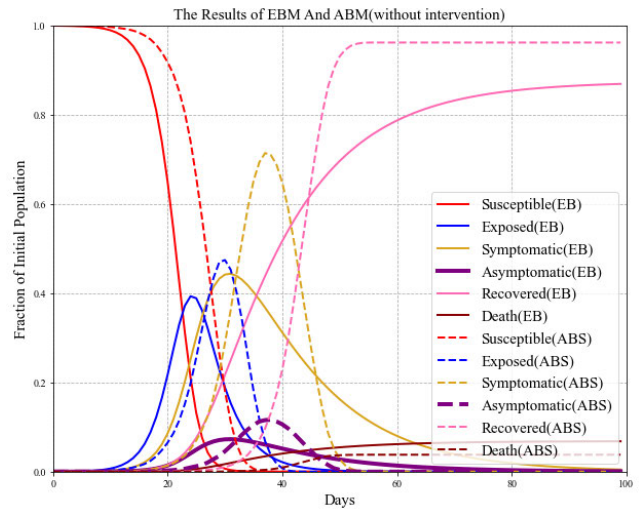


FIGURE 3. The calculation results comparing the ABM with the DES method (ABS) with the equation-based model (EBM) (the vertical axis is the ratio of the case number of each infection state to the whole population, and the horizontal axis is the time).

number of asymptomatic individuals corresponds to a lower success rate of conventional testing methods and a greater likelihood that asymptomatic individuals will not be detected. People who are not screened out will increase the risk of this epidemic spreading.

IV. CONSIDERATION OF VARIOUS EPIDEMIC PREVENTION MEASURES

In this section, the effects of different measures, such as the Contact Tracing Measure (CTM), Location-Based Checking-Testing Measure (LCTM), Lockdown Measure (LM), and Mobile Cabin Isolation and Hospital Measure (MCHM), are calculated by means of this improved ABM. Additionally, the corresponding analysis of the results obtained is also presented.

The pseudocode of our model is given in TABLE 5, which basically describes the process of how our simulation model works.

TABLE 5. Pseudocode of our simulation model.

Algorithm:
Input: The Number of Agents N ; Behavior Pattern Database; The Number of Initial Patients N_0 ;
Output: The Number of All Kinds of People Every Day;
Parameters Setting; $N_0 \leftarrow 3$ (initialization);
Switch (the kind of measure or no measure):
Update the state transition setting;
Update the message triggers setting;
For Day=1 to 100 do:
Agents move or stop according to flow chart;
Interaction among agents by the state diagram;
Update display animation;
Store the state of agents;
Store the output data;
Return the output data.

A. LOCATION-BASED CHECKING-TESTING MEASURE (CTM)

As an infected individual will have an increased body temperature, a quarantine site can be set up for individuals whose body temperature is high. For patients in quarantine sites, nucleic acid testing is used to identify the actual infected individuals, and further medical aid is provided.

The specific measures of this location-based checking policy could be implemented not only with body temperature testing but also with random nucleic acid tests or other combinations of tests to improve the probability of screening out patients. In different locations, even if the same testing technique is used, the outcome may not be the same. However, to simplify the model, we assume that the probability of successfully screening out patients in all different locations is the same.

Based on the premise of the capacity of quarantine facilities $c_{isolation} = 100$ and the capacity of clinics/hospitals $c_{treat} = 50$, we analyzed the dissemination of viruses under different COVID-19 test success rates b_{tc} . For the convenience of comparison, we take the number of recovered individuals (symbolized as R) after 100 days as a benchmark, with a greater R corresponding to better effectiveness of this set of parameter values.

From the simulation results in TABLE 6, the following conclusions can be drawn:

TABLE 6. Simulation results for 10 times with different b_{ct} values.

b_{ct}	0	0.2	0.4	0.6	0.8	1
Experiment 1	17175	17177	17143	17151	17126	17091
Experiment 2	17167	17191	17145	17179	17144	17197
Experiment 3	17146	17145	17204	17166	17167	17152
Experiment 4	17180	17160	17126	17132	17194	17163
Experiment 5	17159	17167	17174	17136	17144	17184
Experiment 6	17143	17129	17174	17135	17146	17150
Experiment 7	17119	17155	17145	17198	17136	17108
Experiment 8	17181	17152	17218	17142	17169	17131
Experiment 9	17105	17182	17124	17163	17163	17200
Experiment 10	17096	17160	17102	17140	17153	17115
AVERAGE	17147	17162	17156	17154	17154	17149

1) Raising b_{tc} increases the number of recovered people. However, under a specific isolation capacity and hospital capacity, the epidemic prevention effect of this measure is obviously still relatively limited. Because each quarantine site or hospital has a limited capacity, once the capacity is exceeded, dysfunction of the medical system will occur.

2) When $b_{tc} < 0.3$, a larger b_{tc} corresponds to a smaller R , indicating that if $c_{isolation}$ and c_{treat} do not match and only increase b_{tc} , the effect of this measure will be limited.

3) When $b_{tc} = 0.6$ or 0.8 , R is clearly the same. The cost of epidemic control required to reach such a screening level is substantial. Even when $b_{tc} = 1$, every person coming in and

out of each subregion must undergo the nucleic acid test at the entry and exit ports of that subregion. The limited capacity for isolation and treatment cannot support superabundant people who may be sick (some people who are screened out may be only close contacts), which will result in collapse of the local quarantine and medical systems and a reduced number of recovered people.

To balance protection and cost, the quarantine capacity and hospital capacity within a region must be considered. For any enclosed region, sufficient $c_{isolation}$ and c_{treat} are more important than a superfluous ability to detect patients.

B. MOBILE CABIN ISOLATION AND HOSPITAL MEASURE (MCHM)

For a given region, $c_{isolation}$ and c_{treat} cannot change significantly within a short time, especially when the COVID-19 success testing rate increases and the effectiveness of plague control does not increase. Thus, the MCHM may be a better option.

Taking this campus as an example, an empty place can be chosen to reform as a temporary isolation location and hospital, with the fundamental aim of elevating the $c_{isolation}$ (as listed in TABLE 4, this implies the capacity of the isolation location) and c_{treat} (as listed in TABLE 4, this implies the capacity of the locations for curing people, includes clinics, hospitals and so on). Various combinations of parameters are tested, such as the quarantine capacity and hospital capacity under $b_{tc} = 0.8$, and all runs are repeated 50 times to compare R after 100 days.

Fig. 4 shows that increasing $c_{isolation}$ or c_{treat} can indeed increase R , but the ratio of $c_{isolation}$ to c_{treat} seems more decisive. When $c_{treat} = 100$ and $c_{isolation}$ increases from 100 to 400, R first increases to 17163 and then decreases to 17151. Among these parameter combinations, R may not increase as $c_{isolation}$ and c_{treat} increase. Although taking MCHM can obviously increase R , the superfluous $c_{isolation}$ and c_{treat} are not helpful for increasing the effect of the MCHM for epidemics. The best parameter combination is $c_{isolation}/c_{treat} = 2$. As shown in Fig. 4, the number of recovered individuals (R) with $c_{isolation} = 800$ and $c_{treat} = 200$ is slightly larger than the number of recovered individuals (R) when $c_{isolation} = 200$ and $c_{treat} = 100$. Although increasing $c_{isolation}$ and c_{treat} can truly increase the number of recovered individuals, the effect of additional capacity can be negligible when $c_{isolation}$ reaches 800 and c_{treat} reaches 400. When fixing $c_{isolation}$ to 800, the days to delay when $c_{treat} = 200$ equals the days when $c_{treat} = 400$, indicating that the major reason for the delay in the peak of the epidemic is the capacity of isolation places, not the capacity of clinics or hospitals to cure patients.

In conclusion, appropriately increasing the capacity of isolation places and places for treatment by establishing mobile cabin isolation and hospitals is a good choice, and increasing the capacity properly can maximize the effectiveness of MCHMs. To ease panic and delay the peak to allow a sufficient reaction time for related organizations, expanding

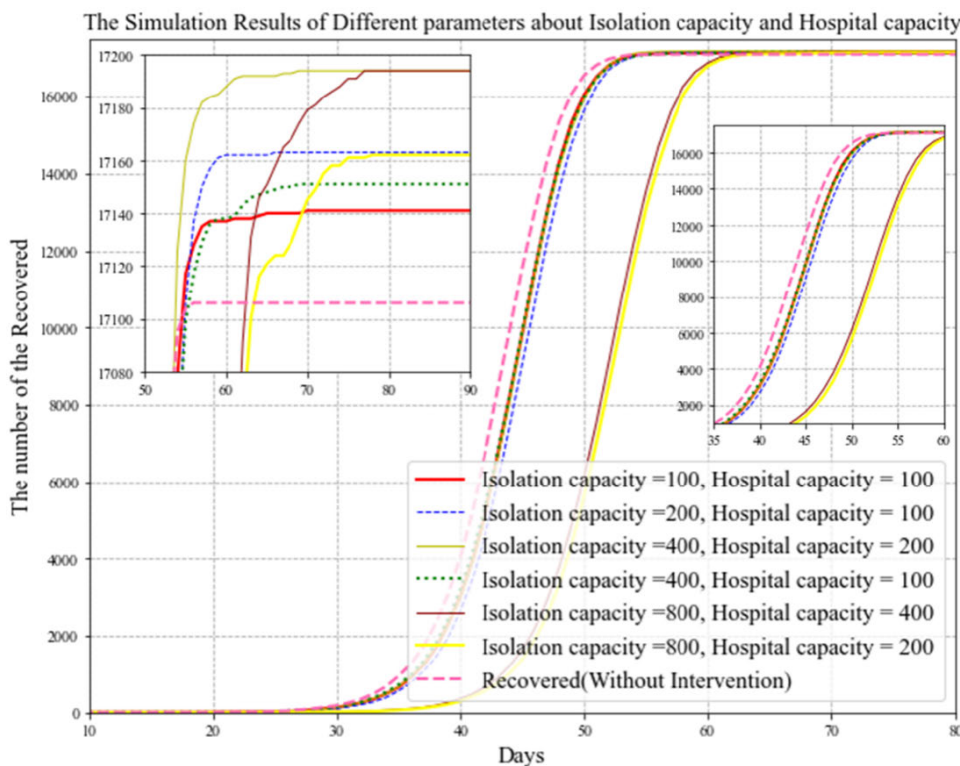


FIGURE 4. Simulation results with different isolation capacities and hospital capacities.

the capacity of isolation places by several times is a viable option even if lacking sufficient c_{treat} .

C. CONTACT TRACING MEASURE (CTM)

For patients identified by temperature screening, nucleic acid testing or other methods, contact tracing measures are implemented to trace people who ever had contact with them. For convenience, this procedure is named the “contact tracing measure” (CTM).

The COVID-19 test success rate $b_{tc} = 0.8$, the capacity for treatment $c_{treat} = 100$, and the capacity of isolation places $c_{isolation} = 400$.

According to the comparison results in Fig. 5, implementing the CTM can only delay an outbreak. In particular, the increasing number of asymptomatic patients attracted our attention. Conventional testing methods, such as temperature screening, cannot be guaranteed or detect all asymptomatic patients if nucleic acid tests are not performed. Perhaps the additional number of asymptomatic patients will increase the risk and difficulty of epidemic control. In other words, asymptomatic cases may evade common detection methods and cause a new outbreak.

D. LOCKDOWN MEASURE (LM)

Eilersen and Sneppen [22] stated that targeted tracking and isolation strategies are better than a long-term lockdown strategy from a cost-benefit perspective. Therefore, in this chapter,

we focus on a cost-benefit comparison between long-term and intermittent LM.

When $c_{isolation} = 400$, $c_{treat} = 100$ and $b_{tc} = 0.8$, the simulation results of a long-term lockdown strategy, targeted tracking and isolation strategy (CTM), and a short-term-but-repetitive lockdown measure (LM) are recorded. The strategy called the short-term-but-repetitive lockdown measure assumes that the duration of the lockdown measure is not long, and a gap exists between the two lockdown durations. However, a long-term lockdown measure implies that the lockdown continues until the end of the epidemic once it starts.

In this paper, these strategies are set as follows. The long-term lockdown strategy will be executed immediately once an outbreak occurs (here, the decision point is set as the time when the number of symptoms reaches 100 for convenience). For the short-term and repetitive LM, the isolation start time was set on the 16th day. After lockdown for 14 days, the region will open, and another 14-day lockdown starts again after an additional 16 days. The average simulation results of 50 independent runs are shown in Fig. 6.

Fig. 6 shows that the short-term repetitive lockdown strategy has the best effect on increasing the number of recovered individuals but has the worst performance on delaying an outbreak. The CTM and long-term LM together have the same effect on delaying the peak of an outbreak and are both better than the CTM alone. Notably, short-term-but-repetitive LM or long-term LM increases the risk of increasing the number

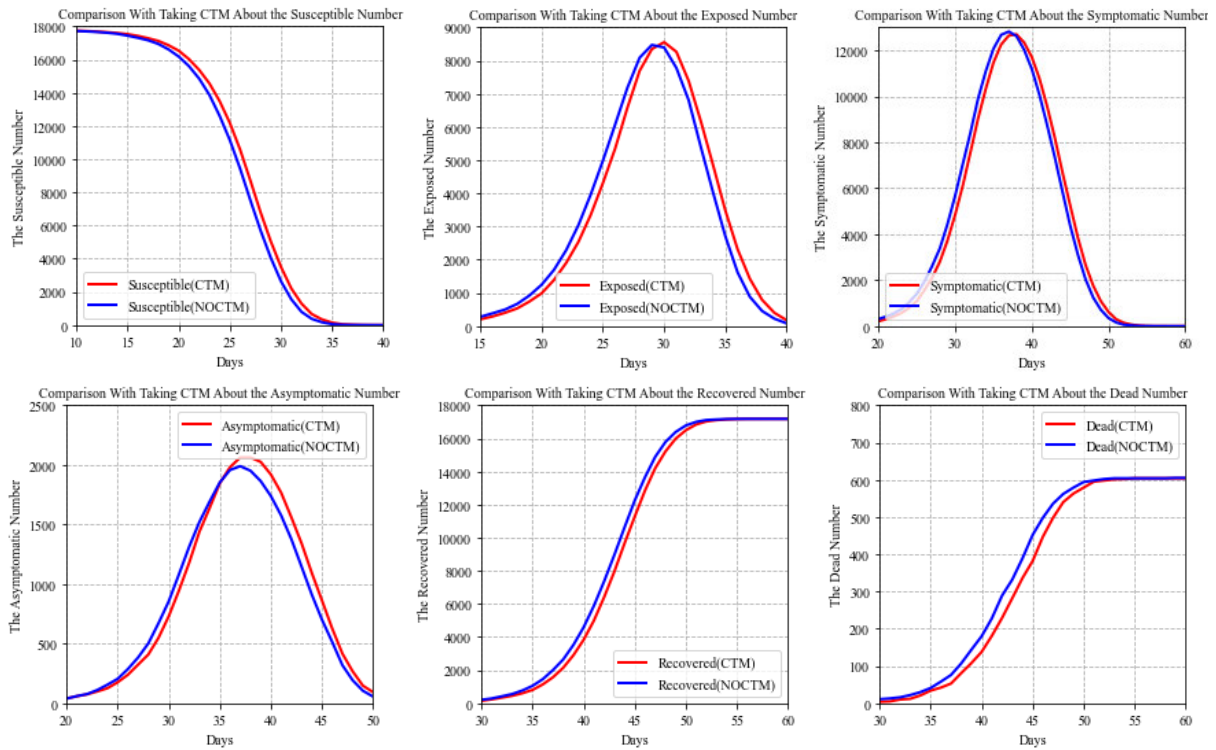


FIGURE 5. Simulation result comparison using Contact Tracing Measure with Taking No Measure.

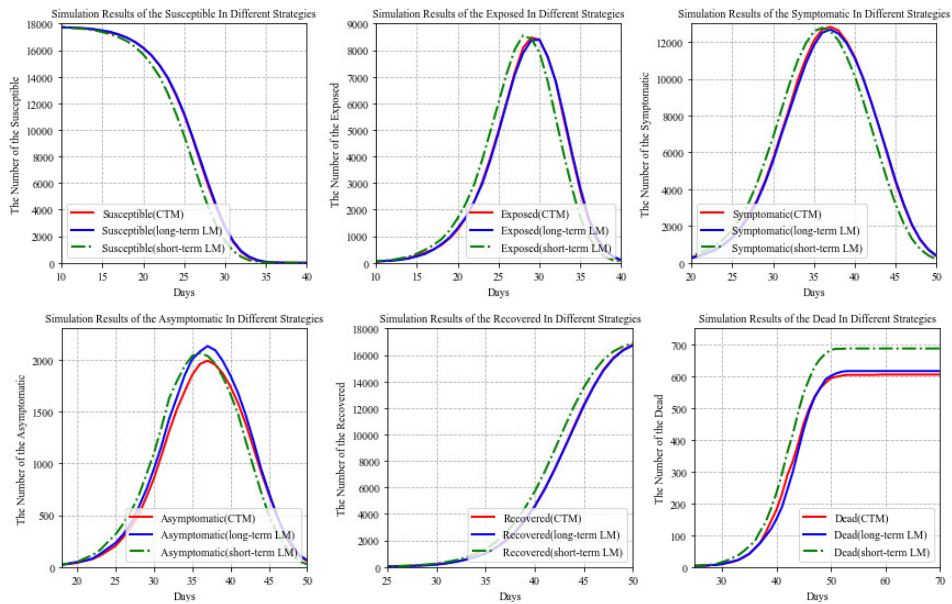


FIGURE 6. Simulation results with three strategies.

of asymptomatic patients. In particular, long-term LM has the highest probability of resulting in a second outbreak. Above all, compared with lockdown measures, tracing measures are better if only to reduce the risk of asymptomatic infection.

Based on the simulation results of the short-term LM, we want to study whether the effect of this measure can be further improved. A 16-day lockdown interval and a 14-day

freeze interval are set to study the further influence. A fixed time interval as a criterion for deciding whether to lockdown or unfreeze is discussed as follows.

A fixed set of parameter values is studied. As the improved ABM (combined with the DES) implements these measures through an event-triggered response, the meaning of lockdown and unfreezing naturally refers to the time when the LM

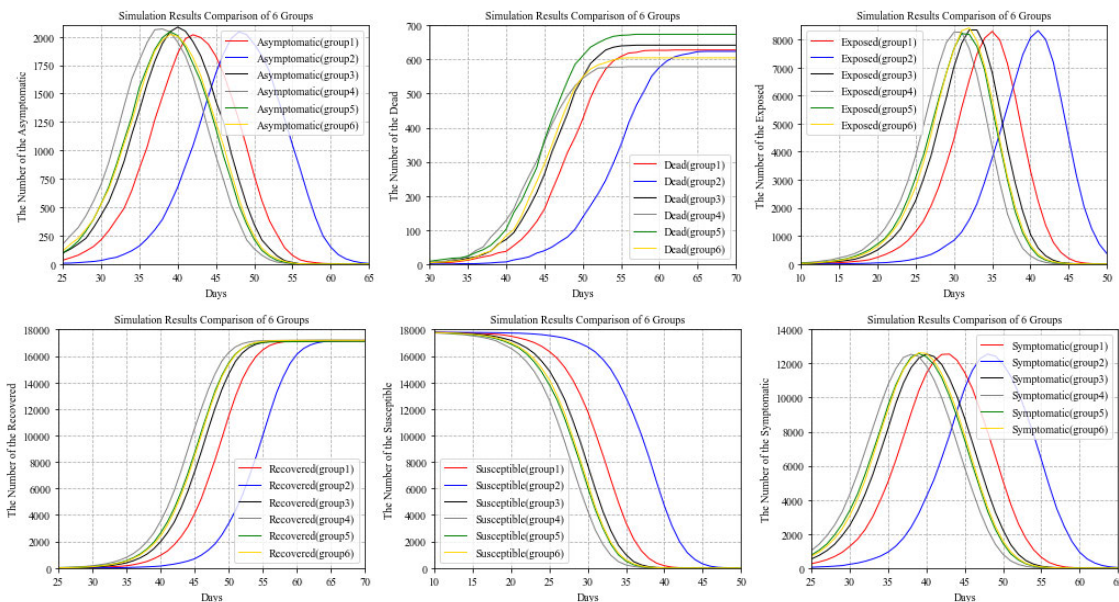


FIGURE 7. Simulation result comparison of 6 groups.

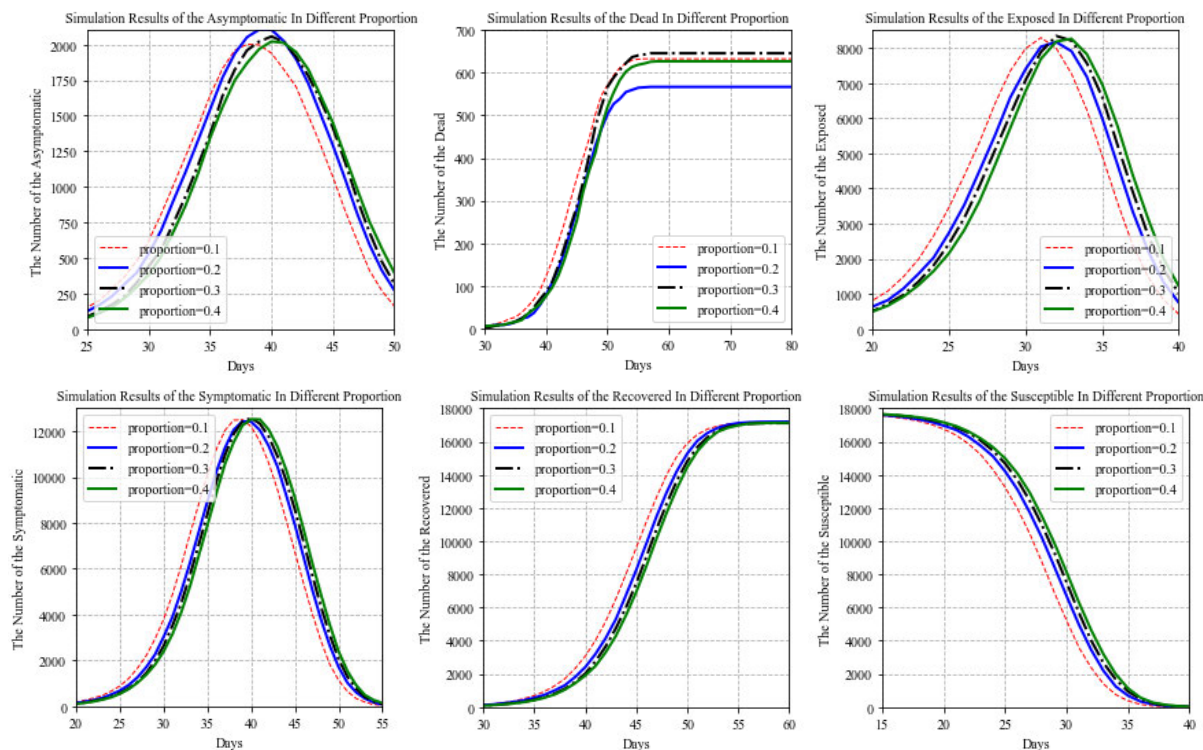


FIGURE 8. Simulation results at different proportions.

is implemented and removed, respectively. Here, 6 groups are set: (1) the first lockdown time is 5 days and the interval to lockdown or unfreeze is 7 days; (2) the first lockdown time is 10 days and the interval to lockdown or unfreeze is 7 days; (3) the first lockdown time is 10 days and the interval to lockdown or unfreeze is 14 days; (4) the first lockdown time is 15 days and the interval to lockdown or unfreeze is 7 days; (5) the first lockdown time is 20 days and the interval

to lockdown or unfreeze is 7 days; and (6) the first lockdown time is 20 days and the interval to lockdown or unfreeze is 14 days. To find the best fixed time interval, various combinations are tested, $c_{isolation} = 400$, $c_{treat} = 100$ and $b_{tc} = 0.8$, and the simulation results are presented in Fig. 7, which are the average simulation results of 50 independent runs.

Short-term repetitive lockdown strategies can be concluded to only delay the onset of an outbreak, especially the peak

of an epidemic. Approximately 10 days later, for the second group, the first lockdown time was 10 days, and the interval between the two lockdown durations was 7 days. The decreasing number of deaths indicates that this strategy has some effect. Fig. 7 indicates that setting the starting time to 10 days is best when the disease is just beginning to spread. The interval between two lockdown durations should be as short as possible.

Then, taking the symptomatic proportion as the standard for deciding whether to lockdown or unfreeze is discussed. The ratio of the number of symptoms to the total number $ratio = I/N$ is set as the trigger to start the lockdown measure. When simulating repeatedly for 50 runs with a $ratio$ ranging from 0.2 to 0.8, the average values are calculated, which are given in Fig. 8. The lockdown measure with different proportions can be observed to have a similar effect on the number of recovered R . Among these, when the proportion is 20%, this measure can yield the best result according to the final number of deaths.

V. CONCLUSION

Agent-based models are very useful in the epidemic prevention field. However, these models are time-consuming and rely on high computing power. Hence, we proposed an improved ABM that is combined with the DES method for improved application. The number of concurrent responses is reduced, which markedly improves its application. The proposed simulation method, which combines the advantages of the ABM and DES, will improve granularity and likelihood estimations in the epidemic prevention field with low concurrence.

Future research can explore how to combine our improved ABM with the GIS technique and improve its fineness [44], [45]. The simulation results reflect the possibility of a second COVID-19 outbreak with only nonpharmaceutical epidemic prevention measures.

REFERENCES

- [1] L. Zou, F. Ruan, M. Huang, L. Liang, H. Huang, Z. Hong, J. Yu, M. Kang, Y. Song, and J. Xia, "SARS-CoV-2 viral load in upper respiratory specimens of infected patients," *New England J. Med.*, vol. 382, no. 12, pp. 1177–1179, Mar. 2020.
- [2] (2020). *COVID-19 Dashboard by the Center for Systems Science and Engineering (CSSE) at Johns Hopkins University*. [Online]. Available: <https://www.arcgis.com/apps/opsdashboard/index.html#/bda7594740fd40299423467b48e9ecf6>
- [3] World Health Organization. (2020). *WHO Declares COVID-19 Disease to be a Pandemic*. [Online]. Available: <https://www.nbcnews.com/health/health-news/live-blog/2020-03-11-coronavirus-news-com1155241>
- [4] S. Tang, Y. Xiao, Z. Peng, and H. Shen, "Prediction modeling with data fusion and prevention strategy analysis for the COVID-19 outbreak," *Chin. J. Epidemiol.*, vol. 41, no. 4, pp. 480–484, 2020.
- [5] E. Volz and L. A. Meyers, "Susceptible-infected-recovered epidemics in dynamic contact networks," *Proc. Roy. Soc. B, Biol. Sci.*, vol. 274, no. 1628, pp. 2925–2934, 2007.
- [6] J. W. Forrester, "System dynamics, systems thinking, and soft or," *Syst. Dyn. Rev.*, vol. 10, nos. 2–3, pp. 245–256, 1994.
- [7] R. Verity, L. Okell, I. Dorigatti, P. Winskill, C. Whittaker, and N. Imai, "Estimates of the severity of coronavirus disease 2019: A model-based analysis," *Lancet Infectious Diseases*, vol. 20, no. 6, pp. 669–677, 2020.
- [8] I. Mahmood, H. Arabnejad, D. Suleimenova, I. Sassooun, A. Marshan, A. Serrano-Rico, P. Louvieris, A. Anagnostou, S. J. E. Taylor, D. Bell, and D. Groen, "FACS: A geospatial agent-based simulator for analysing COVID-19 spread and public health measures on local regions," *J. Simul.*, vol. 10, pp. 1–19, Aug. 2020.
- [9] M. F. Shlesinger, "Complex adaptive systems: An introduction to computational models of social life," *J. Stat. Phys.*, vol. 129, no. 2, pp. 409–410, Oct. 2007.
- [10] M. A. Janssen and E. Ostrom, "Empirically based, agent-based models," *Ecol. Soc.*, vol. 11, no. 2, p. 37, 2006.
- [11] H. J. Holland and H. J. Miller, "Artificial adaptive agents in economic theory," *Amer. Econ. Rev.*, vol. 81, no. 2, pp. 365–370, 1991.
- [12] E. Bruch and J. Atwell, "Agent-based models in empirical social research," *Sociol. Methods Res.*, vol. 44, no. 2, pp. 186–221, May 2015.
- [13] S. Merler, M. Ajelli, L. Fumanelli, M. F. C. Gomes, A. P. Y. Piontti, L. Rossi, D. L. Chao, I. M. Longini, M. E. Halloran, and A. Vespignani, "Spatiotemporal spread of the 2014 outbreak of ebola virus disease in Liberia and the effectiveness of non-pharmaceutical interventions: A computational modelling analysis," *Lancet Infectious Diseases*, vol. 15, no. 2, pp. 204–211, Feb. 2015.
- [14] I. J. M. Mahmood, D. Groen, A. Javed, and F. Shafait, "An agent-based simulation of the spread of dengue fever," in *Computational Science (Lecture Notes in Computer Science)*, vol. 12139. Hampton, NJ, USA: AnyLogic North America, 2020, pp. 103–117.
- [15] E. Hunter, B. Mac Namee, and J. Kelleher, "An open-data-driven agent-based model to simulate infectious disease outbreaks," *PLoS ONE*, vol. 13, no. 12, Dec. 2018, Art. no. e0208775.
- [16] A. T. Crooks and A. B. Hailegiorgis, "An agent-based modeling approach applied to the spread of cholera," *Environ. Model. Softw.*, vol. 62, pp. 164–177, Dec. 2014.
- [17] F. Rakowski, M. Gruzziel, A. Bieniasz-Krzywiec, and J. P. Radomski, "Influenza epidemic spread simulation for Poland—A large scale, individual based model study," *Phys. A, Stat. Mech. Appl.*, vol. 389, no. 16, pp. 3149–3165, Aug. 2010.
- [18] M. Waleed, T.-W. Um, T. Kamal, A. Khan, and Z. U. Zahid, "SIM-D: An agent-based simulator for modeling contagion in population," *Appl. Sci.*, vol. 10, no. 21, p. 7745, Nov. 2020.
- [19] S. Eubank, I. Eckstrand, B. Lewis, S. Venkatramanan, M. Marathe, and C. L. Barrett, "Commentary on Ferguson, et al., 'Impact of non-pharmaceutical interventions (NPIs) to reduce COVID-19 mortality and healthcare demand,'" *Bull. Math. Biol.*, vol. 82, no. 4, Apr. 2020, Art. no. 52.
- [20] M. Cremonini and S. Maghool, "The unknown of the pandemic: An agent-based model of final phase risks," *J. Artif. Soc. Social Simul.*, vol. 23, no. 4, p. 8, 2020.
- [21] A. Gopalan and H. Tyagi, "How reliable are test numbers for revealing the COVID-19 ground truth and applying interventions?" *J. Indian Inst. Sci.*, vol. 100, no. 4, pp. 863–884, Oct. 2020.
- [22] A. Eilersen and K. Sneppen, "Cost-benefit of limited isolation and testing in COVID-19 mitigation," *Sci. Rep.*, vol. 10, no. 1, Dec. 2020, Art. no. 18543.
- [23] J. T. Wu, K. Leung, and G. M. Leung, "Nowcasting and forecasting the potential domestic and international spread of the 2019-nCoV outbreak originating in Wuhan, China: A modelling study," *Obstetrical Gynecol. Surv.*, vol. 75, no. 7, pp. 399–400, Feb. 2020.
- [24] W. Xia, T. Sanyi, C. Yong, F. Xiaomei, X. Yanni, and X. Zongben, "When will be the resumption of work in Wuhan and its surrounding areas during COVID-19 epidemic? A data-driven network modeling analysis," *Scientia Sinica Math.*, vol. 50, no. 7, p. 969, 2020.
- [25] I. M. Longini, "Containing pandemic influenza with antiviral agents," *Amer. J. Epidemiol.*, vol. 159, no. 7, pp. 623–633, Apr. 2004.
- [26] National Health Commission. (2020). *Diagnosis and Treatment Plan for Pneumonia Infected in Novel Coronavirus*. [Online]. Available: <http://www.nhc.gov.cn/zyygj/s7652m/202002/e84bd30142ab4d8982326326e4db22ea.shtml>
- [27] T. Chen, T. Chen, R. Liu, C. Xu, D. Wang, F. Chen, and W. Zhu, "Transmissibility of the influenza virus during influenza outbreaks and related asymptomatic infection in mainland China, 2005–2013," *PLoS ONE*, vol. 11, no. 11, 2017, Art. no. e0166180.
- [28] Y. Huang, Z. Ding, Q. Chen, L. Wu, L. Guo, C. Zhao, L. Sha, and H. Sun, "Environmental virus detection associated with asymptomatic SARS-CoV-2-infected individuals with positive anal swabs," *Sci. Total Environ.*, vol. 753, Jan. 2021, Art. no. 142289.

- [29] A. Borshchev, "Agent based modeling. Technology overview," in *The Big Book of Simulation Modeling: Multimethod Modeling With Anylogic*, vol. 11. Hampton, NJ, USA: AnyLogic North America, Jun. 2013.
- [30] Q. Bi, Y. Wu, S. Mei, C. Ye, X. Zou, Z. Zhang, and X. Liu, "Epidemiology and transmission of COVID-19 in 391 cases and 1286 of their close contacts in Shenzhen, China: A retrospective cohort study," *Lancet Infectious Diseases*, vol. 20, no. 8, pp. 911–919, Apr. 2020.
- [31] K. Mizumoto and G. Chowell, "Transmission potential of the novel coronavirus (COVID-19) onboard the diamond princess cruises ship, 2020," *Infectious Disease Model.*, vol. 5, pp. 264–270, Dec. 2020.
- [32] L. Jia and W. Chen, "Uncertain SEIAR model for COVID-19 cases in China," *Fuzzy Optim. Decis.-Making*, vol. 20, no. 2, pp. 243–259, 2020.
- [33] Z. Yang, Z. Zeng, K. Wang, and S. S. Wong, "Modified SEIR and AI prediction of the epidemics trend of COVID-19 in China under public health interventions," *J. Thoracic Disease*, vol. 2, no. 3, p. 165, 2020.
- [34] T. Murray, J. Garg, and R. Nagi, "Prize collecting multiagent orienteering: Price of anarchy bounds and solution methods," *IEEE Trans. Autom. Sci. Eng.*, early access, Dec. 23, 2020, doi: 10.1109/TASE.2020.3041712.
- [35] S. Agrawal, S. Bhandari, A. Bhattacharjee, and A. Deo, "City-scale agent-based simulators for the study of non-pharmaceutical interventions in the context of the COVID-19 epidemic," *J. Indian Inst. Sci.*, vol. 12, pp. 31–39, Nov. 2020.
- [36] (2021). *Zhejiang University of Technology Admissions*. [Online]. Available: <http://zs.zjut.edu.cn/html/index.html>
- [37] (2021). *Postgraduate Admissions Office of ZJUT*. [Online]. Available: <http://www.yz.zjut.edu.cn/list.asp?tid=6>
- [38] E. Hunter, B. Mac Namee, and J. Kelleher, "A hybrid agent-based and equation based model for the spread of infectious diseases," *J. Artif. Societies Social Simul.*, vol. 23, no. 4, p. 14, 2020.
- [39] V. Grimm, U. Berger, and F. Bastiansen, "A standard protocol for describing individual-based and agent based models," *Ecol. Model.*, vol. 198, pp. 115–126, Dec. 2006.
- [40] N. Marilleau, C. Lang, and P. Giraudoux, "Coupling agent-based with equation-based models to study spatially explicit megapopulation dynamics," *Ecol. Model.*, vol. 384, pp. 34–42, Sep. 2018.
- [41] A. Skvortsov, "Epidemic modeling: Validation of agent-based simulation by using simple mathematical models," in *Proc. Land Warfare Conf.*, 2007, pp. 1–4.
- [42] Defence Science Technology Organization Victoria, Australia. (2020). *Comparison of an Agent-Based Model of Disease Propagation With the Generalised SIR Epidemic Model*. [Online]. Available: <http://citeseerx.ist.psu.edu/viewdoc/download?doi=10.1.1.927.843&rep=rep1&type=pdf>
- [43] J. Li, J. Zhong, Y.-M. Ji, and F. Yang, "A new SEIAR model on small-world networks to assess the intervention measures in the COVID-19 pandemics," *Results Phys.*, vol. 25, Jun. 2021, Art. no. 104283.
- [44] Z. Sun, I. Lorscheid, J. D. Millington, S. Lauf, N. R. Magliocca, J. Groeneveld, S. Balbi, H. Nolzen, B. Müller, J. Schulze, and C. M. Buchmann, "Simple or complicated agent-based models? A complicated issue," *Environ. Model. Softw.*, vol. 86, pp. 56–67, Dec. 2016.
- [45] O. M. Cliff, N. Harding, M. Piraveenan, E. Y. Erten, M. Gambhir, and M. Prokopenko, "Investigating spatiotemporal dynamics and synchrony of influenza epidemics in australia: An agent-based modelling approach," *Simul. Model. Pract. Theory*, vol. 87, pp. 412–431, Sep. 2018.
- [46] Z. Xu and D. YaQiong, "Fatality rate analysis and treatment strategies of COVID-19," *Genomics Appl. Biol.*, vol. 39, no. 9, pp. 4405–4408, 2020.
- [47] J. Mason, "SARS-CoV-2 is a super virus," *Int. J. Super Species Res.*, vol. 10, no. 1, pp. 1–2, 2020.



His research interests include intelligent system planning and intelligent algorithms.



SIRUI DING was born in Taizhou, Jiangsu, China, in 2000. He is currently pursuing the bachelor's degree in industrial engineering with Zhejiang University of Technology. His main research interests include intelligent algorithms and intelligent system planning.



WENCHAO YI (Member, IEEE) received the B.Sc. and Ph.D. degrees in industrial engineering from Huazhong University of Science and Technology, Wuhan, China, in 2011 and 2016, respectively. She is currently a Lecturer with the College of Mechanical Engineering, Zhejiang University of Technology, China. Her current research interests include evolutionary algorithms and their application in scheduling.



RUIFENG LV was born in Nanyang, Henan, China, in 1980. He received the B.S. and M.S. degrees in mechanical engineering from Harbin Institute of Technology, Harbin, and the Ph.D. degree in mechanical engineering from Harbin Institute of Technology, in 2009. Since 2009, he has been a Lecturer with the Institute of Industrial Engineering, Zhejiang University of Technology, Hangzhou. His research interests include intelligent system layout planning and intelligent algorithms.



CHENG WANG received the B.S. degree in industrial engineering from Zhejiang University of Technology, Hangzhou, in 2005, and the Ph.D. degree in systems engineering from Tianjin University, Tianjin, China, in 2010. Since 2016, he has been an Associate Professor with the Institute of Industrial Engineering, Zhejiang University of Technology. His research interests include data-driven decision-making and complex systems.

...



HONGBIN QIU was born in Leqing, Zhejiang, China, in 1998. He received the B.S. degree in industrial engineering from Zhejiang University of Technology, Hangzhou, China, in 2020, where he is currently pursuing the master's degree in agent-based simulation methods and multiagent algorithms.